Conclusion

INDO MO calculations have been useful in pinpointing the substantial variations in $^3J_{FC}$ caused by the number, type, and orientation of substituents which are sufficient to seriously hamper the use of this coupling in the derivation of conformational and configurational information. In particular small couplings require careful consideration before an interpretation in terms of the spatial relationship of the nuclei is attempted. In this context $^3J_{FC}$ displays the same intricacies of detail that are shown by other couplings involving carbon.

Supplementary Material Available: A figure of the correlation of the calculated $^3J_{CH}^{trans}$ (ref 3 and 7) with $^3J_{FC}^{trans}$ (ref 7 and this work) and a comparison of calculated $^3J_{FC}$ values for fluorine substitution in the 1-fluoropropane system with those of similar systems for $^3J_{CH}$ and $^3J_{CC}$ are given; a complete list of the IND-O-FPT results for $^3J_{FC}$ in mono-, di-, tri-, tetra-, and pentamethyl-substituted 1-fluorocyclohexanes, 1-fluoropropane, 1,1-difluoropropane, 1,1,1-trifluoropropane, 1,2-difluoropropane, 1,2,2-trifluoropropane, 1,3-difluoropropane (two conformations), 1,3,3-trifluoropropane (two conformations), 1,3,3,3-tetrafluoropropane, fluoromethyl methyl ether and (fluoromethyl)methylamine (7 pages). Ordering information is given on any current masthead page.

Aspects of Artificial Photosynthesis. Photosensitized Electron Transfer across Bilayers, Charge Separation, and Hydrogen Production in Anionic Surfactant Vesicles

Mohammad S. Tunuli and Janos H. Fendler*

Contribution from the Department of Chemistry, Texas A&M University, College Station, Texas 77843. *Received July 24, 1980*

Abstract: Photosensitized electron transfer from tris(2,2′-bipyridine)ruthenium cation, $Ru(bpy)_3^{2+}$, to methylviologen, MV^{2+}, has been investigated in the presence of negatively charged dihexadecyl phosphate, DHP, surfactant vesicles by steady state photolysis, fluorescence quenching, and nanosecond laser flash photolysis. Four different substrate–surfactant vesicle organizations have been used. In system I, $Ru(bpy)_3^{2+}$ was attached to the outer and MV^{2+} was placed onto the inner surfaces of DHP vesicles. In system II, MV^{2+} was attached to the outer and $Ru(bpy)_3^{2+}$ to the inner surfaces of DHP vesicles. In system III, both $Ru(bpy)_3^{2+}$ and MV^{2+} were localized on the outer surfaces of DHP vesicles. In system IV, both $Ru(bpy)_3^{2+}$ and MV^{2+} were localized on the inner surfaces of DHP vesicles. Extremely efficient electron transfers have been observed on the surfaces of surfactant vesicles in systems III and IV. Electron transfer from excited $Ru(bpy)_3^{2+}$ to MV^{2+} across the bilayers of vesicles in the presence of externally added EDTA in system I resulted in the formation of reduced methylviologen, $MV^{+\cdot}$, up to 75% conversion with a quantum efficiency of 2.40×10^{-2}. If additionally $\sim 10^{-5}$ M PtO_2 was entrapped in the interiors of DHP vesicles in system I, $MV^{+\cdot}$ promptly reformed with concomitant hydrogen evolution. Photolysis of this system leads to the net consumption of only EDTA at very low stoichiometric $Ru(bpy)_3^{2+}$, MV^{2+}, and PtO_2 concentrations. Dynamics of these processes have been determined and their relevance to photochemical solar energy conversions is discussed.

Photochemical energy conversion and storage are extremely active areas of current research.[1-8] Investigations are directed to catalytic sunlight initiated hydrogen production from water. One approach has involved mimicking photosynthesis in grossly simplified chemical systems.[7] Photosynthesis is brought about by the extremely efficient organization of appropriate molecules in the chloroplast.[9] Conceptually, photosynthesis involves four steps: energy deposition, charge separation, electron transfer, and utilization of suitable redox couples.

Completely synthetic surfactant vesicles have been found to be useful media for organizing sensitizers and electron donor–acceptor couples.[10] Sonic dispersal of long-chain dialkyldimethylammonium halides,[11-15] dialkyl phosphates,[16,17] sulfonates, and carboxylates[16] results in vesicle formation. Positively charged dioctadecyldimethylammonium chloride (DODAC) and anionic dihexadecylphosphate (DHP) vesicles have been characterized most extensively.[10] Well sonicated DODAC and DHP give fairly uniform single compartment prolate ellipsoid vesicles with (1–5) $\times 10^7$ dalton molecular weights.[18] These surfactant vesicles have

(1) Calvin, M. *Acc. Chem. Res.* **1978**, *11*, 4701.
(2) Porter, G.; Archer, M. V. *ISR, Interdiscip. Sci. Rev.* **1976**, *1*, 119.
(3) Hautala, R. R.; King, R. B.; Kutal, C. "Solar Energy, Chemical Conversion and Storage"; The Humana Press: Clifton, N.J., 1979.
(4) Bolton, J. R. "Solar Power and Fuels"; Academic Press: New York, 1977.
(5) Archer, M. D. In "Photochemistry, Specialists Periodical Report"; The Chemical Society: London, 1978; Vol. 9, p 603; *Ibid.* 1977; Vol. 8, p 570; *Ibid.* 1976; Vol. 7, p 561; *Ibid.* **1976**; Vol. 6, p 737.
(6) Claesson, S.; Engström, M. "Solar Energy—Photochemical Conversion and Storage"; National Swedish Board for Energy Source Development: Stockholm, 1977.
(7) Barber, J. "Photosynthesis in Relation to Model Systems"; Elsevier: New York, 1979.
(8) Gerischer, H.; Katz, J. J. "Light Induced Charge Separation in Biology and Chemistry"; Verlag Chemie: New York, 1979.
(9) Govindjee "Bioenergetics of Photosynthesis"; Academic Press: New York, 1975.
(10) Fendler, J. H. *Acc. Chem. Res.* **1980**, 13, 7.
(11) Kunitake, K.; Okahata, Y.; Tamaki, K.; Takayanagi, M.; Kumamaru, F. *Chem. Lett.* **1977**, 387.
(12) Kunitake, T.; Okahata, Y. *J. Am. Chem. Soc.* **1977**, *99*, 3890.
(13) Kunitake, T.; Okahata, Y. *Chem. Lett.* **1977**, 1337.
(14) Deguchi, K.; Mino, J. *J. Colloid Interface Sci.* **1978**, *65*, 155.
(15) Tran, C. D.; Klahn, P. L.; Romero, A.; Fendler, J. H. *J. Am. Chem. Soc.* **1978**, *100*, 1622.
(16) Kunitake, T.; Okahata, Y. *Bull. Chem. Soc. Jpn.* **1978**, *51*, 1877.
(17) Mortara, R. A.; Quina, F. H.; Chaimovich, H. *Biochem. Biophys. Res. Commun.* **1978**, *81*, 1080.

0002-7863/81/1503-2507$01.25/0

long-term stabilities in the pH 2–12 range, are osmotically active, undergo thermotropic phase transitions, and, most importantly, entrap and retain molecules in their compartments.[10] Surfactant vesicles possess, therefore, all the advantages of liposomes[19] without their chemical instabilities.

Previously, we have demonstrated efficient energy[20] and electron[21] transfers as well as photoionizations[22] in surfactant vesicles. Particularly interesting has been the observed electron transfer from DODAC vesicle intercalated *N*-methylphenothiazine to photoexcited tris(2,2′-bipyridine)ruthenium^{2+} ion, $Ru(bpy)_3^{2+}$, anchored onto the surface of the vesicles by a long hydrocarbon chain.[21] The *N*-methylphenothiazine radicals formed were readily expelled both into the vesicle entrapped and into bulk water. Electrostatic repulsions between the cation radicals and the positively charged vesicle surface hindered undesirable charge recombinations. Parts of the *N*-methylphenothiazine cation radical which escaped from the vesicle into the bulk aqueous solution survived for extended periods (≫1 ms).[21] Interestingly, judicious addition of sodium chloride profoundly affected the lifetime of the cation radical and its partitioning between the aqueous inner core of the vesicles and bulk water.[21]

An even more beneficial molecular organization is the subject of the present report. Efficient photosensitized electron transfer has been observed across the bilayers of DHP vesicles *in the absence of charge carriers* by steady-state and by nanosecond laser flash photolysis. The sensitizer, $Ru(bpy)_3^{2+}$, and the acceptor, methylviologen, MV^{2+}, were localized separately, either at the inner or at the outer surface of the surfactant vesicles. Visible light-initiated photolysis in the presence of EDTA resulted in the stoichiometric reduction of MV^{2+} to reduced methylviologen, $MV^{+}\cdot$. Trapping of PtO_2 in the inner compartments of DHP vesicles led to hydrogen evolution and to concomitant reoxidation of $MV^{+}\cdot$. Quenching of the excited state $Ru(bpy)_3^{2+}$ by MV^{2+} has also been investigated on the surface of DHP vesicles.

Experimental Section

Dihexadecylphosphate, DHP (Sigma), and disodium ethylenediamine tetraacetate, EDTA (Sigma), were used as received. Tris(2,2′-bipyridine)ruthenium chloride, $Ru(bpy)_3^{2+}$ (Strem Chemicals), was recrystallized from water. Methylviologen chloride, MV^{2+} (Sigma), was recrystallized from cold methanol by adding acetone and platinum oxide (Adam's catalyst), PtO_2 (Tridom), was used as received.

Steady state irradiations were carried out by using an Oriel 450 W Xenon lamp in conjunction with a 400-nm cutoff filter. Thermostated and stirred solutions (5.0 mL) were degassed by argon purging prior to (20 min) and during the photolysis. Development of the photoproducts was monitored by taking absorption spectra on a Cary 118-C spectrophotometer. The photon flux was determined by means of a ferrioxalate chemical dosimeter to be 2.66×10^{16} quanta/s.[23] Mass spectrometric analysis was carried out on a Hewlett-Packard Model 5980A mass spectrometer.

Steady state fluorescence excitation and emission spectra were obtained on a Spex Fluorolog Spectrofluorimeter with the use of the E mode. Front face angle illumination was used to minimize inner filter effects. Generally, 2–5-mm slits and a 10-nm bandwidth were used.

The computer controlled nanosecond nitrogen (337 nm) laser flash photolysis system has been described.[24] Transients were observed under an atmosphere of nitrogen gas at ambient temperature.

Surfactant vesicles were prepared by the sonic dispersal of DHP, using the microtip of a Braunsonic 1510 sonifier set at 70 W. Typically sonications were carried out at 80 °C for 30 min. The four different DHP vesicle systems, illustrated in Figure 1, were prepared as follows.

System I. DHP (5.0 mg) was dispersed in 2.0 mL triply distilled water for 5 min at 80 °C prior to adding the required amounts of methylviologen stock solution (in triply distilled water). This step prevented fusion. Sonication of the MV^{2+}-containing DHP vesicle solution continued for an additional 25 min at 80 °C at a 70 W setting. The resultant vesicle solution was passed through a Bio-Rad Ag-50W-X2 cation exchange column (proton form, 200–400 mesh). This removed MV^{2+} from the bulk solution and from the outer surface of the vesicles. The concentration of MV^{2+}, entrapped in the DHP vesicles, was determined spectrophotometrically, taking $\epsilon_{270\,nm}$ for $MV^{2+} = 1.4 \times 10^4$ M^{-1} cm^{-1}. The absence of MV^{2+} on the outer surface and in the bulk solution was demonstrated by the addition of sodium dithionite. No blue color, due to reduced MV^{2+} ($MV^{+}\cdot$), was produced. Addition of MeOH (~1 cm^3) resulted in the destruction of the surfactant vesicle and in the prompt development of blue color (due to $MV^{+}\cdot$). Concentration of $MV^{+}\cdot$ was determined by using $\epsilon_{295\,nm} = 3.8 \times 10^4$ M^{-1} cm^{-1} or $\epsilon_{603\,nm} = 1.24 \times 10^4$ M^{-1} cm^{-1} for $MV^{+}\cdot$. In all cases good agreement was found between measurements of MV^{2+} and $MV^{+}\cdot$. Appropriate amounts of $Ru(bpy)_3^{2+}$ stock solution were added to MV^{2+}-containing DHP vesicles.

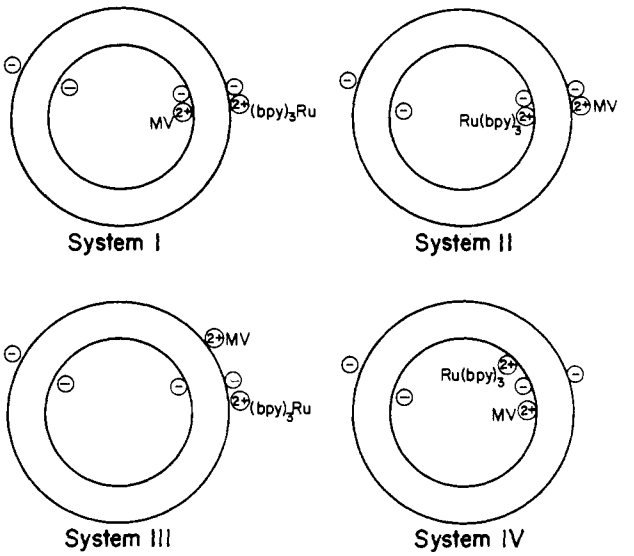

Figure 1. Schematics of the different DHP surfactant vesicle–sensitizer–acceptor systems used.

PtO_2-containing system I was prepared by dispersing 5.0 mg of DHP and 0.3 mg of PtO_2 in 2.0 mL of triply distilled water at 80 °C prior to adding the required amounts of MV^{2+}. Sonication continued for an additional 25 min. Unentrapped PtO_2 was separated by centrifugation (15 min on a table-top model). The resultant solution was passed through a cation exchange column and appropriate amounts of $Ru(bpy)_3^{2+}$ were added as described above. The stoichiometric concentration of vesicle entrapped PtO_2 is estimated to be 10^{-6} M. For mass spectroscopic analysis solutions were prepared by dispersing 5.0 mg of DHP and 0.3 mg of PtO_2 in 2.0 mL of D_2O. Passing through the cation exchange resin (equilibrated in H_2O) and adding the appropriate concentrations of $Ru(bpy)_3^{2+}$ as described above resulted in a PtO_2-containing system I containing 60% D_2O.

System II consists of negatively charged DHP surfactant vesicles in which MV^{2+} is attached to the outer and $Ru(bpy)_3^{2+}$ is attached to the inner surfaces (Figure 1). System II was prepared analogously to System I; $Ru(bpy)_3^{2+}$ rather than MV^{2+} was cosonicated with sonicated DHP. Evidence for the presence of $Ru(bpy)_3^{2+}$ within the DHP vesicles was obtained by observing identical (corrected for volume changes) absorption spectra of solution prior and subsequent to a passage throught the ion exchange resin. No absorption due to $Ru(bpy)_3^{2+}$ was observed in the eluents. MV^{2+} was added subsequent to passing the $Ru(bpy)_3^{2+}$ solutions through the ion exchange resin.

System III. DHP (5.0 mg) was dispersed in 2.0 mL of triply distilled water for 30 min at 80 °C. The vesicle solution was then passed through the cation exchange column in the same manner as described for system I. Appropriate amounts of $Ru(bpy)_3^{2+}$ and MV^{2+} were added to the already formed vesicles. System III consists, therefore, of DHP vesicles in which *both* $Ru(bpy)_3^{2+}$ and MV^{2+} are attached electrostatically to the outer surface (Figure 1).

System IV. DHP (5.0 mg) was dispersed in 2.0 mL of triply distilled water for 15 min at 80 °C prior to the addition of appropriate amounts of MV^{2+} and $Ru(bpy)_3^{2+}$. Subsequent to the addition of these cations sonication continued for another 15 min. The resultant solution was passed through the cation exchange resin in the same manner described for system I. System IV consists, therefore, of negatively charged DHP vesicles in which *both* $Ru(bpy)_3^{2+}$ and MV^{2+} are electrostatically atta-

(18) Herrmann, U.; Fendler, J. H. *Chem. Phys. Lett.* **1979**, *64*, 270.
(19) Gregoriadis, G.; Allison, A. C. "Liposomes in Biological Systems"; Wiley: New York, 1980.
(20) Nomura, T.; Escabi-Perez, J. R.; Sunamoto, J.; Fendler, J. H. *J. Am. Chem. Soc.* **1980**, *102*, 1484.
(21) Infelta, P. P.; Gratzel, M.; Fendler, J. H. *J. Am. Chem. Soc.* **1980**, *102*, 1479.
(22) Escabi-Perez, J. R.; Romero, A.; Lukac, S.; Fendler, J. H. *J. Am. Chem. Soc.* **1979**, *101*, 2231.
(23) Calvert, J. G.; Pitts, J. N. "Photochemistry"; Wiley: New York, 1966.
(24) Lindig, B. A.; Rodgers, M. A. J. *J. Phys. Chem.* **1979**, *83*, 1683.

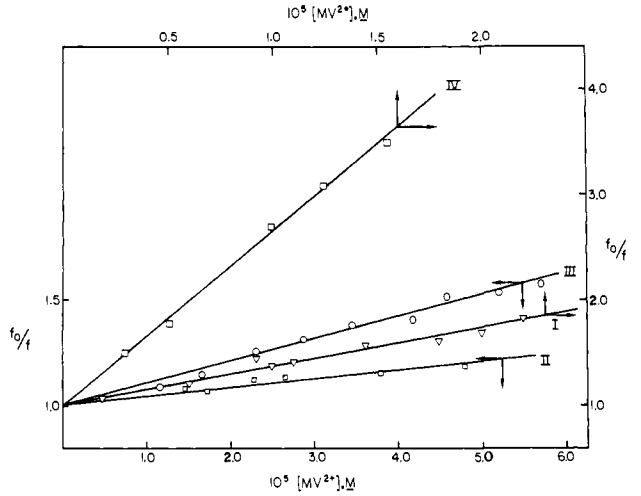

Figure 2. Stern-Volmer plots for the quenching of $Ru(bpy)_3^{2+}$ luminescence intensity in the different DHP vesicle systems by methylviologen. Stoichiometric concentrations of $Ru(bpy)_3^{2+}$ and MV^{2+} are given in Table I. See Figure 1 for definitions of the systems.

ched to the inner surface (Figure 1). The pHs of all systems were adjusted to 8.4 by aqueous NaOH (2-3 drops). Stoichiometric concentrations of $Ru(bpy)_3^{2+}$ and MV^{2+} in the different vesicle systems were determined by absorption spectrophotometrically taking $\epsilon_{270\,nm} = 2.0 \times 10^4\ M^{-1}\ cm^{-1}$ and $\epsilon_{450\,nm} = 1.4 \times 10^4\ M^{-1}\ cm^{-1}$ for $Ru(bpy)_3^{2+}$ and $\epsilon_{270\,nm} = 1.4 \times 10^4\ M^{-1}\ cm^{-1}$ and $\epsilon_{450\,nm} = 2.1 \times 10^0\ M^{-1}\ cm^{-1}$ for MV^{2+}.

Results

Luminescence Quenching. Steady state excitation of 1.2×10^{-5} M $Ru(bpy)_3^{2+}$, in surfactant vesicles prepared from 9.0×10^{-3} M stoichiometric DHP at 450 nm, resulted in an emission spectrum similar to that observed in aqueous solution.[25] Addition of MV^{2+}, even at a concentration as low as 2.0×10^{-6} M, quenched the luminescence of $Ru(bpy)_3^{2+}$. This quenching in the ranges of MV^{2+} concentration shown in Figure 2 obeyed the Stern-Volmer equation. The very nature of surfactant vesicles[10] limits the concentrations of the sensitizers and acceptors. Thus, 1.55×10^{-5} M MV^{2+} and 1.0×10^{-5} M $Ru(bpy)_3^{2+}$ were the highest possible concentrations of quencher and sensitizer that could be entrapped in the interior of DHP vesicles in system IV. Addition of $Ru(bpy)_3^{2+}$ (system I), MV^{2+} (system II), or both (system III) in concentrations $\geq 10^{-4}$ to already formed vesicles caused partial neutralization of the negative charges on the outer surface of DHP vesicles. This, in turn, promoted vesicle to vesicle fusion, manifested in turbidity changes and ambiguous quenching. Addition of MV^{2+} or $Ru(bpy)_3^{2+}$ in excess of 10^{-4} M increased turbidities and resulted ultimately in precipitations and breaks in the Stern-Volmer plots. Table I summarizes conditions, the Stern-Volmer quenching constants, K_{sv} values, and quenching rate constants, k_q values, obtained for the quenching of $Ru(bpy)_3^{2+}$ luminescence by MV^{2+} in the different systems.

Steady State Photolysis. Irradiation of deoxygenated solutions containing MV^{2+} at the inner and $Ru(bpy)_3^{2+}$ at the outer surfaces of DHP vesicles (system I) with visible light ($\lambda \geq 400$ nm) resulted in the prompt development of a blue color in the presence of EDTA. Figure 3 shows absorption changes in a typical irradiation experiment. The development of absorption maxima at 395 and 600 nm is characteristic for the formation of reduced methylviologen, $MV^{+\cdot}$.[28] In the absence of air, $MV^{+\cdot}$ persisted for hours. Introduction of air into the cuvette resulted in the prompt reoxidation of $MV^{+\cdot}$ to MV^{2+} as manifested by decolorization. Acidification (to pH 1), under an atmosphere of N_2, had also

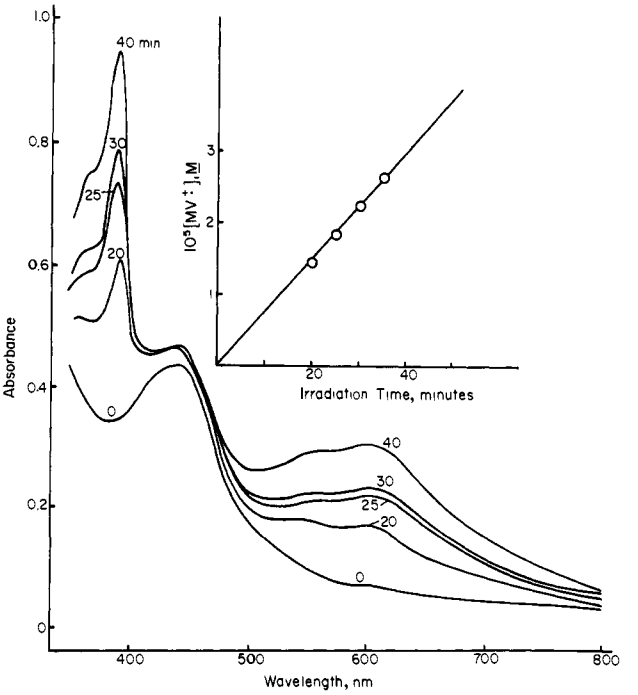

Figure 3. Absorption spectra of system I + EDTA (added to already formed vesicles) prior to and 20, 25, 30, and 40 min after irradiation with visible light (using a 450 W Xenon lamp and 400 nm cutoff filter). Stoichiometric concentrations: [DHP] = 2.4×10^{-3} M; [$Ru(bpy)_3^{2+}$] = 3.0×10^{-5} M; [MV^{2+}] = 4.05×10^{-5} M; [EDTA] = 1.0×10^{-3} M at pH 8.4. The insert shows the buildup of $MV^{+\cdot}$ as a function of irradiation time.

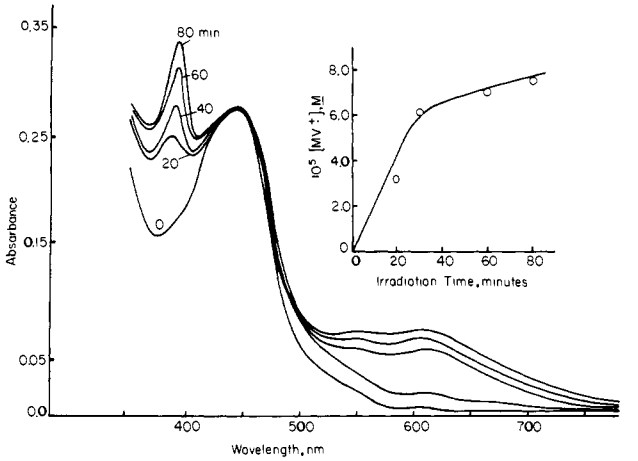

Figure 4. Absorption spectra of system III + EDTA (added to already formed vesicles) prior to and 20, 30, 60, and 80 min after irradiation with visible light (using a 450 W Xenon lamp and a 400 nm cutoff filter). Stoichiometric concentrations: [DHP] = 2.4×10^{-3} M; [$Ru(bpy)_3^{2+}$] = 1.9×10^{-5} M; [MV^{2+}] = 1.0×10^{-5} M; [EDTA] = 1.0×10^{-3} M, pH 8.4. The insert shows the buildup of $MV^{+\cdot}$ as a function of irradiation time.

destroyed the blue color. This latter experiment is indicative of hydrogen formation. Hydrogen and deuterium formation was, in fact, determined by mass spectrometry in irradiated PtO_2 containing D_2O solutions of system I. This unambiguously demonstrates, of course, that deuterium originates from the photosensitized decomposition of D_2O rather than from hydrogen possibly adsorbed on the catalyst.[30] Decomposition of EDTA does not give rise to H_2. The absorption spectra of reoxidized solutions were identical with those prior to photolysis. Taking $\epsilon_{603\,nm} = 1.24 \times 10^4\ M^{-1}\ cm^{-1}$,[31] concentrations of $MV^{+\cdot}$ formed

(25) Meisel, D.; Matheson, M. S.; Rabani, J. *J. Am. Chem. Soc.* **1978**, *100*, 117.
(26) Gaines, G. L., Jr. *J. Phys. Chem.* **1979**, *83*, 3088.
(27) Schmell, R. H.; Whitten, D. G. *J. Am. Chem. Soc.* **1980**, *102*, 1938.
(28) Rodgers, M. J.; Becker, J. C. *J. Phys. Chem.* **1980**, *84*, 2762.
(29) Matsuo, T.; Nagamura, T.; Itoh, K.; Nishijima, T. *Mem. Fac. Eng. Kyushu Univ.* **1980**, *40*, 25.
(30) Lehn, J. M.; Sauvage, J. P. *Nouv. J. Chim.* **1977**, *1*, 449.
(31) Ford, W. E.; Otvos, J. W.; Calvin, M. *Nature (London)* **1978**, *274*, 509.

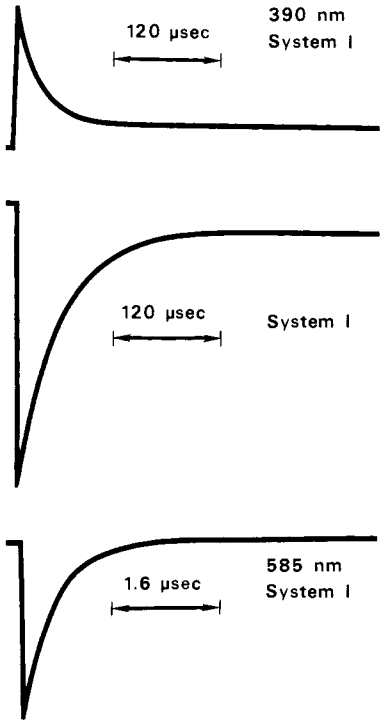

Figure 5. Transient absorbances due to $MV^{+}\cdot$ at 390 nm, bleaching of $Ru(bpy)_3^{2+}$ at 450 nm and luminescence decay at 585 nm following excitation (by a 337 nm, 20 ns laser pulse) of system I. Stoichiometric concentrations: [DHP] = 5.0×10^{-3} M; $[Ru(bpy)_3^{2+}] = 9.9 \times 10^{-5}$; $[MV^{2+}] = 5.8 \times 10^{-4}$ M.

are plotted as a function of irradiation time in the insert of Figure 3. Sensitized photoreduction of MV^{2+} is an efficient process. The amount of $MV^{+}\cdot$ formed increased linearly with irradiation time, up to 75% conversion in system I. The quantum efficiency for this process was determined to be 1.04×10^{-3} at a photon flux of 2.99×10^{16} quanta/s. Passing the excitation light through a 0.25-m Jarrell-Ash monochromator caused similar high percentages of photoconversion, although necessarily at much slower rates than that shown in the insert of Figure 3.

Irradiation of deoxygenated solutions containing *both* $Ru(bpy)_3^{2+}$ and MV^{2+} at the outer surfaces of DHP vesicles (system III) with visible light ($\lambda \geq 400$ nm) also resulted in the development of a blue color in the presence of EDTA (Figure 4). Qualitatively, photosensitized $MV^{+}\cdot$ formation was found to be similar in systems I and III. The process is much less efficient, however, in the latter system (see Discussion). As shown in the insert of Figure 4, $MV^{+}\cdot$ formation is only linear with irradiation time up to 10% conversion. Similarly, the determined quantum efficiency for $MV^{+}\cdot$ formation in system III was only 1.34×10^{-4} at the same photon flux.

No $MV^{+}\cdot$ was produced in either systems I or III in the dark or in the absence of $Ru(bpy)_3^{2+}$. No buildup of $MV^{+}\cdot$ could be detected in the steady state photolysis of system IV.

Laser Flash Photolysis. Excitation of deoxygenated solutions containing MV^{2+} at the inner and $Ru(bpy)_3^{2+}$ at the outer surfaces of DHP vesicles (system I) with a 20 ns, 337 nm laser pulse resulted in the bleaching of the ground state absorption, at 450 nm, and in the appearances of a transient absorption with a maximum at 390 nm and of a luminescence with an emission maximum at 585 nm. This behavior is readily rationalized by the transfer of an electron from excited state $Ru(bpy)_3^{2+}$, $Ru(bpy)_3^{2+*}$, to MV^{2+}:

$$Ru(bpy)_3^{2+} \xrightarrow{h\nu} Ru(bpy)_3^{2+*} \quad (1)$$

$$Ru(bpy)_3^{2+*} + MV^{2+} \xrightarrow{k_2} Ru(bpy)_3^{3+} + MV^{+}\cdot \quad (2)$$

Figure 5 illustrates typical digitized tracings for the decay of $MV^{+}\cdot$ at 390 nm, for the recovery of the ground state absorption of $Ru(bpy)_3^{2+}$ at 450 nm, and for the decay of $Ru(bpy)_3^{2+*}$ luminescence at 585 nm in system I. Typically, excitation by a single

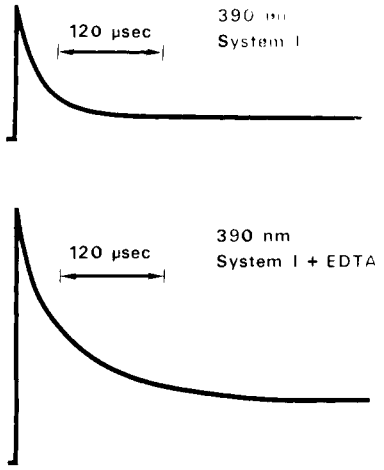

Figure 6. Transient absorption changes due to $MV^{+}\cdot$ at 390 nm following excitation (by a 337 nm, 20 ns laser pulse) of system I in the absence and in the presence of 1.1×10^{-3} M EDTA (added to already formed vesicles). Stoichiometric concentrations: [DHP] = 5.0×10^{-3} M; $[Ru(bpy)_3^{2+}] = 9.9 \times 10^{-5}$; $[MV^{2+}] = 5.8 \times 10^{-4}$ M. Differences in initial intensities are the consequences of using different incident intensities of laser beam.

laser pulse results in the formation of 2×10^{-7} M $MV^{+}\cdot$ (i.e., about 0.2% conversion). Luminescence decays were observed to follow first-order kinetics, having rate constants in the $(1-3) \times 10^6$ s^{-1} range. The half-lifetime of the luminescence decay in system I containing $[Ru(bpy)_3^{2+}] = 9.9 \times 10^{-5}$ M and $[MV^{2+}] = 5.8 \times 10^{-5}$ (Figure 5), for example, was 0.31 μs. This corresponded with the buildup (not shown) of $MV^{+}\cdot$.

Both the decay of $MV^{+}\cdot$ and the recovery of $Ru(bpy)_3^{2+}$ absorbance are second-order processes having half-lifetimes in the order of 30–50 μs. Using $\epsilon_{395} = 3.8 \times 10^4$ M^{-1} cm^{-1} for $MV^{+}\cdot$[31,32] and $\epsilon_{450} = 1.4 \times 10^4$ M^{-1} cm^{-1} for $Ru(bpy)_3^{2+}$ in combination with the slopes of the second-order plots and with the optical path length of the cell (4.0 mm), apparent rate constants for the decay of $MV^{+}\cdot$ and that for the recovery of the $Ru(bpy)_3^{2+}$ bleaching in system I were calculated to be 4×10^{10} and 1.5×10^{10} M^{-1} s^{-1}, respectively. The similarity of these two rate constants is explicable in terms of the reformation of both MV^{2+} and $Ru(bpy)_3^{2+}$:

$$Ru(bpy)_3^{3+} + MV^{+}\cdot \xrightarrow{k_3} Ru(bpy)_3^{2+} + MV^{2+} \quad (3)$$

It should be emphasized that these apparent rate constants were calculated on the basis of stoichiometric reagent concentrations. In reality, all the cationic reagents are localized on the negative surfaces of DHP vesicles and, therefore, their concentrations are at least four orders of magnitude higher than the stoichiometric values. Consequently, the "true" rate constants for k_3 are in the order of 10^6 M^{-1} s^{-1}. Importantly, a fraction of $MV^{+}\cdot$ survives for milliseconds and longer (Figure 5).

Steady state photolysis showed that in deoxygenated system I (or III) $MV^{+}\cdot$ persisted for hours in the presence of externally added EDTA (vide supra). Flash photolysis experiments nicely substantiate this observation. The amount of $MV^{+}\cdot$ persisting for a long time is appreciably greater in the presence of EDTA than in its absence (Figure 6). The function of EDTA is to remove $Ru(bpy)_3^{3+}$:

$$Ru(bpy)_3^{3+} + EDTA \xrightarrow{k_4} Ru(bpy)_3^{2+} + EDTA_{oxidized} \quad (4)$$

thereby preventing the back reaction (eq 3).

The quantum efficiency for $MV^{+}\cdot$ formation, η, in the laser flash photolysis experiments was estimated from:[33]

$$\eta = \Phi_{Ru(bpy)_3^{2+}\cdot}\eta_q\eta_{tr} \quad (5)$$

where $\Phi_{Ru(bpy)_3^{2+}\cdot}$, η_q, and η_{tr} are the quantum yield for the for-

(32) Kalayanasundaram, K. *J. Chem. Soc., Chem. Commun.* **1978**, 628.
(33) Kalayanasundaram, K.; Kiwi, J.; Grätzel, M. *Helv. Chim. Acta* **1978**, *61*, 2720.

Table I. Quenching of $Ru(bpy)_3^{2+}$ by MV^{2+} in Different Media

medium	stoichiometric concn		K_{sv}, M^{-1}	$10^{-9}k_q$, M^{-1} s^{-1} [a]	ref
	$[Ru(bpy)_3^{2+}]$, M	$[MV^{2+}]$, M			
system I[b]	1.2×10^{-5}	$(2\text{–}20) \times 10^{-6}$	3.6×10^4	115	this work
system II[b]	9.2×10^{-6}	$(1\text{–}5) \times 10^{-5}$	4.2×10^3	14	this work
system III[b]	1.0×10^{-5}	$(1\text{–}6) \times 10^{-5}$	1.0×10^4	400	this work
system IV[b]	1.0×10^{-5}	$(3\text{–}15) \times 10^{-6}$	1.6×10^5	530	this work
H_2O			1.08×10^2	0.2	26
aqueous micellar SDS[c]	1.5×10^{-5}	$(0.2\text{–}2.0) \times 10^{-3}$	1.5×10^3	4.4	27
aqueous micellar CTAB	1.5×10^{-5}	$(0.2\text{–}2.0) \times 10^{-3}$	<1	0.002	27, 28
reversed micellar aerosol-OT/heptane				<0.001	28
liposome[c]	1.5×10^{-5}	2×10^{-2}	<0.1	<0.01[d]	29

[a] Calculated from $k_a = K_{sv}/\tau_0$, where τ_0 is the fluorescence lifetime. Estimated errors are ±15%. [b] See Figure 1 for definitions; stoichiometric concentrations used. Quenching and rate constants are apparent values, therefore. [c] Using a surfactant analogue of $Ru(bpy)_3^{2+}$. [d] Upper limit.

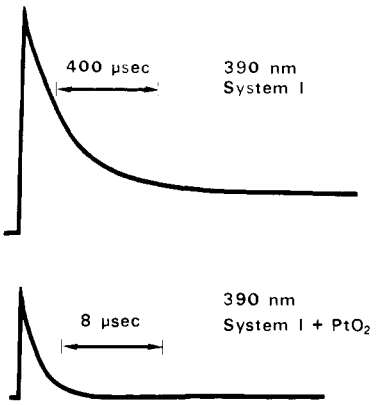

Figure 7. Transient absorption changes due to $MV^{+\cdot}$ at 390 nm following excitation (by a 337 nm, 20 ns laser pulse) of system I in the absence and in the presence of PtO_2 (localized in the interior of vesicles). Stoichiometric concentrations: [DHP] = 5.0×10^{-3} M; $[Ru(bpy)_3^{2+}] = 9.2 \times 10^{-5}$ M; $[MV^{2+}] = 4.5 \times 10^{-4}$ (no PtO_2); 3.8×10^{-4} (in presence of 10^{-5} M PtO_2).

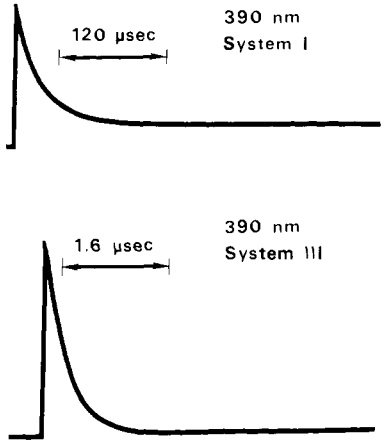

Figure 8. Transient absorption changes due to $MV^{+\cdot}$ at 390 nm following excitation (by a 337 nm, 20 ns laser pulse) of systems I and III. Stoichiometric concentrations for system I: [DHP] = 5.0×10^{-3} M; $[Ru(bpy)_3^{2+}] = 9.9 \times 10^{-5}$ M; $[MV^{2+}] = 5.8 \times 10^{-4}$ M. Stoichiometric concentrations for system III: [DHP] = 5.0×10^{-3} M; $[Ru(bpy)_3^{2+}] = 9.9 \times 10^{-5}$ M; $[MV^{2+}] = 5.8 \times 10^{-4}$ M.

mation of the metal to ligand charge transfer excited state of the ruthenium complex, the probability of quenching, and the charge transfer events, respectively. The term $\Phi_{Ru(bpy)_3^{2+\cdot}}$ is practically unity[34] and η_{tr} is taken to be 0.25.[32] The probability of $Ru(bpy)_3^{2+*}$ quenching by MV^{2+} is given by:

$$\eta_q = \frac{k_2[MV^{2+}]}{k_2[MV^{2+}] + k_0} \qquad (6)$$

where k_0 is rate constant for the luminescence decay in the absence of quencher. Using stoichiometric MV^{2+} concentrations (5.8×10^{-4} M) and assuming homogeneous kinetics, we determined that $\eta_q = 0.096$. Substituting into eq 5, we obtained a quantum efficiency of 2.40×10^{-2} for $MV^{+\cdot}$ formation. In view of the approximations involved this value should not be considered anything but an indication of the order of magnitude of the quantum efficiency.

Steady state photolysis of system I containing PtO_2 in the inner compartments of DHP vesicles was shown to result in catalytic hydrogen evolution (vide supra). The amount of PtO_2 used in the present experiments was so small that it did not increase the turbidity of surfactant vesicles. This condition favored the dynamic investigations of PtO_2 mediated reoxidation of $MV^{+\cdot}$ by laser flash photolysis.[35] Figure 7 compares the transient decay of $MV^{+\cdot}$ in system I in the absence and in the presence of $\sim 10^{-5}$ M PtO_2. In the presence of PtO_2, the half-lifetime of $MV^{+\cdot}$ decreases from ~ 50 μs to 0.9 μs. Significantly, no residual absorbance was seen at 390 nm 16 μs after the laser pulse (Figure 7). Furthermore, the kinetics of $MV^{+\cdot}$ decay changed from a second-order process in the absence of PtO_2 to a first-order process in the presence of PtO_2. These observations are entirely consistent with the Pt-promoted $MV^{+\cdot}$ reoxidation and coupled water reduction:

$$2MV^{+\cdot} + H_2O \xrightarrow[Pt]{k_7} H_2 + 2OH^- + 2MV^{2+} \qquad (7)$$

The rate constant was determined to be $k_7 = 7.7 \times 10^5$ s^{-1}.

The back reaction (eq 3) is dramatically more facile if both the sensitizer and the acceptor are localized at the outer surface of the negatively charged DHP vesicle (system III). Figure 8 compares the transient decays of $MV^{+\cdot}$ at 390 nm in systems I and III. In contrast to system I, $MV^{+\cdot}$ decayed completely 2 μs after the laser pulse. Further, the kinetics of $MV^{+\cdot}$ decay changed from a second-order process in system I to a first-order process in system III. The rate constant for reaction 3 in system III was determined to be $k_3 = 3 \times 10^6$ s^{-1}.

Under our experimental conditions, we could not observe the transient formation of $MV^{+\cdot}$ in system IV.

No $MV^{+\cdot}$ was detected in either systems I or III in the absence of $Ru(bpy)_3^{2+}$.

Discussion

Electron Transfer on the Surfaces of Surfactant Vesicles. Quenching of the $Ru(bpy)_3^{2+*}$ luminescence by MV^{2+} in systems III and IV is extremely efficient. Apparent Stern–Volmer quenching constants are 2–3 orders of magnitude greater than that found in water (Table I). Strong electrostatic interactions between the negatively charged phosphate headgroups and the positively charged sensitizers and acceptors results in effective bindings of both $Ru(bpy)_3^{2+}$ and MV^{2+} at the surface of DHP vesicles. Sites of electron transfer quenching are, therefore, the outer (in System III) or the inner (in System IV) surfaces of DHP vesicles. In this circumstance, the apparent enhanced $Ru(bpy)_3^{2+*}$

(34) Boletta, F.; Maestri, M.; Balzani, J. *J. Phys. Chem.* **1976**, *80*, 2499.
(35) Kiwi, J.; Grätzel, M. *Nature (London)* **1979**, *281*, 657. Kiwi, J.; Grätzel, M. *J. Am. Chem. Soc.* **1979**, *101*, 7214.

quenching is the consequence of grossly increased effective MV^{2+} concentration in the potential field of DHP vesicles. Apparent rate constants for scavenging of the 2,2,5,5-tetramethyl-1-pyrrolidinyloxy-3-carboxylate spin probe, R^-; by sodium ascorbate in the presence of cationic dioctadecyldimethylammonium chloride, DODAC, vesicles has been found to be 20-fold faster than that in water.[36] Taking into consideration the reagent concentration localized within the potential field of the vesicles resulted, in fact, in some sevenfold lower rate constants for the scavenging of R^- than that occurring in homogenous aqueous solutions.[36]

Electron transfer is likely to occur by diffusion or hopping on the vesicle surface. Under the experimental conditions of steady state quenching (stoichiometric [DHP] = 9×10^{-3} M; [$Ru(bpy)_3^{2+}$] = 1×10^{-5} M; [MV^{2+}] = $(1-6) \times 10^{-5}$ M; [DHP vesicle] = 1.6×10^{-7} M[18]), 62 molecules of $Ru(bpy)_3^{2+}$ and 310 molecules of MV^{2+} associate with each DHP vesicle. Taking charge repulsions into consideration average areas for $Ru(bpy)_3^{2+}$ and MV^{2+} are estimated to be 400 and 200 Å^2, respectively. Since the surface area of a DHP vesicle is 12×10^6 Å^2,[18] the maximum area the reactive partners need to cover prior to collision is only 200 Å^2. This value is orders of magnitude smaller than the 10^5 Å^2 estimated for $\bar{d}^2$, the square of the mean diffusive displacement of $Ru(bpy)_3^{2+}$ and MV^{2+}.[28] The maximum area the reactive partners travel is even smaller at the higher concentrations of reagents used in the laser experiments in system III (Figure 8). Thus, reactive partners can readily find each other on the surface of DHP within their lifetimes. Naturally, the close proximity results in much enhanced back reaction (reaction 3, Figure 8). A similar situation has been encountered on the surface of anionic micellar sodium dodecyl sulfate.[28,37,38] In 8.2×10^{-2} M surfactant the observed rate constant ($k_3 = 5.7 \times 10^6$ s^{-1})[28] is remarkably similar to that found in system III ($k_3 = 3.0 \times 10^6$ s^{-1}). The decay of $MV^{+\cdot}$ follows first order rather than second order kinetics on the surfaces of both negatively charged DHP vesicles and aqueous micelles.[28,37,38] Close proximity of the reaction partners and their electrostatic attraction to the surface of the vesicle precludes intervesicle exchanges.[27] Fast intramicellar reactions have been shown to be pseudo-first-order processes.[39,40]

Much smaller stoichiometric concentrations of MV^{2+} could be accommodated on the inner than on the outer surface of DHP vesicles (Table I). Nevertheless, under the experimental conditions used essentially all of the charges on the DHP vesicles are neutralized by entrapped $Ru(bpy)_3^{2+}$ and MV^{2+}. The confinement of reagents in the restricted inner volume of the surfactant vesicle manifests in much enhanced reactivities for reactions 2 and 3. The back reaction is so fast in system IV that it could not detected under our experimental conditions. A similar situation has been found in reversed micelles.[28] Reactive partners are likely to be so close to each other on the inner surface of DHP vesicles that they need not diffuse prior to reaction. Electron transfers become, therefore, less than three-dimensional processes. Reduction of dimensionality is an important means to bring about ultrafast processes in solids and on membrane surfaces.[40-44]

Electron Transfer across Surfactant Vesicle Bilayers. The most significant result of the present study is the direct demonstration of efficient electron transfer from $Ru(bpy)_3^{2+*}$ across the bilayers of surfactant vesicles to MV^{2+} in the absence of charge carriers.

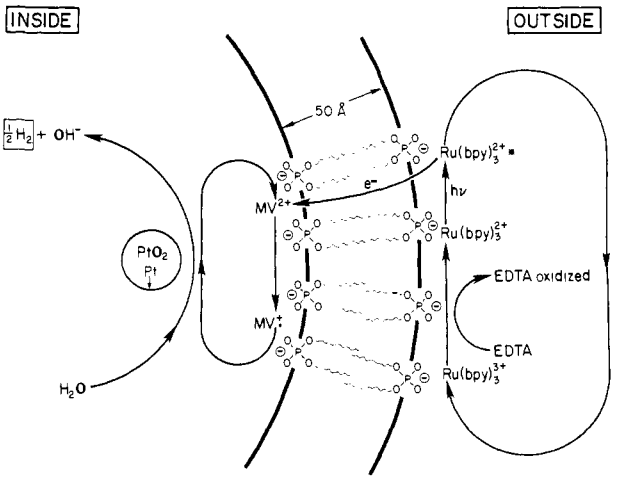

Figure 9. Schematic of the surfactant vesicle system used for the photosensitized catalytic hydrogen production, resulting only in the consumption of EDTA.

Localization of sensitizers on the outer surface and MV^{2+} in the interior of DHP vesicles (system I) proved to be most favorable. In the presence of external EDTA the $MV^{+\cdot}$ formed increased linearly with increased irradiation time up to 75% conversion with a quantum efficiency of 2.40×10^{-2} (Results). This system differs markedly from those previously studied in phospholipid liposomes.[45,46] Specifically, in Calvin's system a surfactant derivative of $Ru(bpy)_3^{2+}$ was anchored by its long chain to *both* the inner and outer surface and EDTA was placed in the inner volume of single compartment egg yolk liposomes while heptylviologen, C_7V^{2+}, was dissolved in the continuous aqueous phase.[45] Photolysis with visible light resulted in $C_7V^{+\cdot}$ formation after a pronounced induction period. The quantum yield became maximal after 1% conversion of C_7V^{2+} and it decreased to about one-fifth of the maximum after 10% reduction.[45] In an analogous organization of the dodecyl derivative of $Ru(bpy)_3^{2+}$ and dodecyl viologen, $C_{12}V^{2+}$, in dipalmitoylphosphatidylcholine liposomes dimers of $C_{12}V^{+\cdot}$ formed and the quantum efficiency for $C_{12}V^{2+}$ reduction was only 10% of that found in micellar hexadecyltrimethylammonium chloride.[46]

Separating $Ru(bpy)_3^{2+}$ and MV^{2+} by some 50 Å on the opposite sides of DHP vesicles, electrostatic bindings and favorable potential gradients are believed to be responsible for the efficiency of the present system. In System I all the negative charges on the inner surface of DHP vesicles are neutralized by MV^{2+}, whereas there is only partial neutralization on the outer surface by $Ru(bpy)_3^{2+}$. The potential gradient created facilitates the flow of electrons from the outer to the inner surface of the vesicle. The situation is quite different in system II. Vesicle–vesicle fusion precludes extensive coverage of the outer surface of DHP vesicles by MV^{2+}. The obtainable potential gradient is much smaller, therefore, than that in system I.

Flip–flop of $Ru(bpy)_3^{2+}$ or MV^{2+} across the bilayers of DHP vesicles is unlikely at the time scales investigated. No MV^{2+} was found to migrate to the outside in system I (see Results). Flip–flop of substrates in liposomes occurs at the time scale of days.[47] Reduction of MV^{2+} is the consequence, therefore, of electron transfer rather than sensitizer–quencher encounter. Electron transfer has been observed in lecithin matrices between molecules separated by as much as 30 Å.[48] Alternatively, electron tunnelling has been proposed in some vesicles.[49-52] The present data are

(36) Lim, Y. Y.; Fendler, J. H. *J. Am. Chem. Soc.* **1979**, *101*, 4023.
(37) Meisel, D.; Matheson, M. S.; Rabani, J. *J. Am. Chem. Soc.* **1978**, *100*, 111.
(38) Rodgers, M. A. J.; Foyt, D. C.; Zimek, Z. A. *Radiat. Res.* **1978**, *75*, 296.
(39) Infelta, P. P.; Grätzel, M. *J. Chem. Phys.* **1979**, *70*, 179.
(40) Hatlee, M. D.; Kozak, J. J.; Rothenberger, G.; Infelta, P. P.; Grätzel, M. *J. Phys. Chem.* **1980**, *84*, 1508.
(41) Escabi-Perez, J. R.; Fendler, J. H. *J. Am. Chem. Soc.* **1978**, *100*, 2234.
(42) Adam, G.; Delbrück, M. In "Structural Chemistry and Molecular Biology"; Rich, A.; Davidson, N., Eds.; W. A. Freeman and Co.: San Francisco, Calif., 1968.
(43) Richter, P. H.; Eigen, M. *Biophys. Chem.* **1974**, *2*, 225.
(44) Eigen, M. In "Quantum Statistical Mechanics in the Natural Sciences"; Kuseneglu, B.; Mintz, S. C.; Widmayer, S., Eds.; Plenum Press: New York, 1974; p 37.
(45) Ford, W. E.; Otvos, J. W.; Calvin, M. *Proc. Natl. Acad. Sci. USA* **1979**, *76*, 3590.
(46) Matsuo, T.; Takamura, K.; Tsutsui, Y.; Nishijima, T. *J. Coord. Chem.* **1980**, *10*, 187.
(47) Jain, M. K.; White, H. B. *Advan. Lipid Res.* **1977**, *15*, 1.
(48) Beddard, G. S.; Porter, G.; Weese, G. M. *Proc. R. Soc. London, Ser. A* **1975**, *A342*, 317.
(49) Kuhn, H. *J. Photochem.* **1979**, *10*, 111.
(50) Van Huevelen, A. *J. Biol. Phys.* **1974**, *1*, 215.
(51) Ilani, A.; Berns, D. S. *Biophysik (Berlin)* **1973**, *9*, 209.

insufficient for distinguishing between these and other alternatives for the mechanism of electron transfer.

Entrapping PtO_2 in the interior of DHP vesicles of system I resulted in the prompt reoxidation of $MV^{+}\cdot$ (Figure 7). The rate constant for this process at ca. 10^{-6} M PtO_2 concentration, $k_7 = 7.7 \times 10^5$ s^{-1}, is an order of magnitude greater than that reported previously for using 1.25×10^{-3} M poly(vinyl alcohol) stabilized colloidal platinum in aqueous solutions.[35] Apparently, very small amounts of PtO_2, localized in the inner pools of DHP vesicles, provide superior catalytic powers and obviate the need for polymer stabilization[35] in order to observe the dynamics of platinum mediated catalysis. Dispersed PtO_2 have large catalytic surfaces and act as microelectrodes.[53-55] Photolysis of PtO_2 carrying DHP vesicles of system I leads to the net consumption of only EDTA. Figure 9 shows the schematics of the hydrogen generating system.

An important feature of the present system is the extremely low concentration of sensitizer ($Ru(bpy)_3^{2+}$), acceptor (MV^{2+}), and catalysts (PtO_2) used. Comparable aqueous systems utilized several orders of magnitude higher concentrations of these components with much less efficiency.[30,33,46,56-60] Currently we are determining hydrogen and deuterium yields quantitatively under various experimental conditions and continue to exploit surfactant vesicles to mimic photosynthesis.

Acknowledgment. Support of this work by the National Science Foundation and by the Department of Energy is gratefully acknowledged. Laser experiments were carried out at the Center for Fast Kinetics Research, University of Texas, Austin. This facility is supported by NIH Grant RR-00886 from the Biotechnology Branch of the Division of Research Resources and by the University of Texas. We benefited from helpful discussions with Dr. Michael A. J. Rodgers. M.S.T. thanks the Pakistan Ministry of Education for financial support and Gomal University, D.I.K., for study leave. Work reported here will form part of the dissertation submitted by M.S.T. for the degree of Doctor of Philosophy at Texas A&M University.

(52) Mangel, M. *Biochim. Biophys. Acta* **1976**, *430*, 459.
(53) Bockris, J. O'M.; Srinavasan, S. *Electrochim. Acta* **1964**, *9*, 71.
(54) Kita, H. *J. Electrochem. Soc.* **1966**, *113*, 1095.
(55) Schuldiner, S.; Warner, T.; Piersma, B. *J. Electrochem. Soc.* **1967**, *114*, 343.
(56) Moradpour, A.; Amoyal, E.; Keller, P.; Kagan, H. *Nouv. J. Chim.* **1978**, *2*, 574.
(57) Brow, G.; Brunschwig, B.; Creutz, C.; Endicott, J.; Sutin, N. *J. Am. Chem. Soc.* **1979**, *101*, 1298.
(58) DeLaive, P.; Sullivan, B.; Meyer, T.; Whitten, D. *J. Am. Chem. Soc.* **1979**, *101*, 4007.
(59) Krasna, A. *Photochem. Photobiol.* **1979**, *29*, 267.
(60) McLendon, G.; Miller, D. S. *J. Chem. Soc., Chem. Commun.* **1980**, 533.

Solid State Disproportionation Enthalpies

Gerald R. Stevenson* and Steven S. Zigler

Contribution from the Department of Chemistry, Illinois State University, Normal, Illinois 61761. *Received September 11, 1980. Revised Manuscript Received November 17, 1980*

Abstract: Using calorimetric techniques, we have measured the heats of reaction of several solid anion radical and dianion salts with water. These heats of reaction have been coupled in a thermochemical cycle to yield the first enthalpies of disproportionation for anion radicals in the solid phase. The enthalpies of disproportionation ($\Delta H°$ for $2Na^+A^-\cdot(s) \rightleftarrows Na^+{}_2A^{2-}(s) + A(s)$) range from −13.6 when A is pyrene to +8.8 kcal/mol when A represents tetracene. The enthalpy of disproportionation for the pyrene salt is the most exothermic anion radical disproportionation yet reported and is largely controlled by the crystal lattice energies of the dianion and anion radical salts.

The equilibria of radical anion disproportionation in solution have been extensively studied,[1-8] and mostly through the efforts of Szwarc and co-workers[1-6] a rather complete picture has been developed explaining anion radical disproportionation in molecular terms. The effects of solvation and ion association fit consistently into this picture.

Despite the extensive work on disproportionation in solution, not a single report has appeared concerning anion radical disproportionation in the solid state. Solid state anion radical disproportionation cannot be studied via equilibria measurements due to the very long reaction times that are necessary to reach an equilibrium state. These very long reaction times are due to the very slow migration of electrons and counterions between crystals of anion radical ($M^+A^-\cdot$), dianion ($M^+{}_2A^{2-}$), and neutral species (A). The kinetic problems can be circumvented by the use of calorimetric methods. Here we wish to report the first enthalpies of anion radical disproportionation in the solid state, eq 1.

$$2M^+A^-\cdot(s) \rightarrow A(s) + M^+{}_2A^{2-}(s) \quad (1)$$

Experimental Section

Tetrahydrofuran (THF) solutions of the anion radical or dianion of polyacene hydrocarbons were generated via the reduction of the polyacene with an equal molar or a large excess of sodium metal, respectively.[9,10] After complete formation of the anion radical or dianion salts

(1) (a) Roberts, R. C.; Szwarc, M. *J. Am. Chem. Soc.* **1965**, *87*, 5542. (b) Rainis, A.; Szwarc, M. *Ibid.* **1974**, *96*, 3008. (c) Cserhegyi, A.; Jagur-Grodzinski, J.; Szwarc, M. *Ibid.* **1969**, *91*, 203. (d) Lundgren, B.; Levin, G.; Claesson, S.; Szwarc, M. *Ibid.* **1975**, *97*, 262. (e) Levin, G.; Szwarc, M. *Ibid.* **1976**, *48*, 4211.
(2) (a) Levin, G.; Szwarc, M. *Chem. Phys. Lett.* **1975**, *35*, 323. (b) Pola, J.; Levin, G.; Szwarc, M. *J. Phys. Chem.* **1976**, *80*, 1690. (c) Levin, G.; Holloway, B. E.; Szwarc, M. *J. Am. Chem. Soc.* **1976**, *98*, 5707.
(3) Levin, G.; Claesson, S.; Szwarc, M. *J. Am. Chem. Soc.* **1972**, *94*, 8672.
(4) Degroof, B.; Levin, G.; Szwarc, M. *J. Am. Chem. Soc.* **1977**, *99*, 474.
(5) Wang, H. C.; Levin, G.; Szwarc, M. *J. Am. Chem. Soc.* **1977**, *99*, 5056.
(6) Jachimowicz, F.; Wang, H. C.; Levin, G.; Szwarc, M. *J. Phys. Chem.* **1978**, *82*, 1371.
(7) Levin, G.; Holloway, B. E.; Mao, C. R.; Szwarc, M. *J. Am. Chem. Soc.* **1978**, *100*, 5841.
(8) Stevenson, G. R.; Williams, E.; Caldwell, G. *J. Am. Chem. Soc.* **1979**, *101*, 520.
(9) Stevenson, G. R.; Wiedrich, C. R. *J. Am. Chem. Soc.* **1979**, *101*, 5092.

0002-7863/81/1503-2513$01.25/0